

Fault systems impede incision of the Yarlung river into the Tibetan plateau

Dongxu Cai¹, Xianyan Wang^{1,2✉}, Guangwei Li^{3✉}, Ruohong Jiao⁴, Barry Kohn⁵, Wenbin Zhu³, Johan De Grave⁶ & Huayu Lu¹

It is widely accepted that tectonics generally enhances river incision. However, why rivers have not incised further into orogenic plateaus to destroy terrains over long-time scales remains ambiguous. Here we hypothesize that the diverse nature of regional tectonics could have impeded river erosion, taking Yarlung River in Tibetan Plateau as a case. We constrain the incision history and effect of a tectonic rift on fluvial incision by low-temperature thermochronology. Results show focused cooling near the rift, but markedly reduced cooling in the upstream and downstream regions since ~7 Ma. This coincides with an episode of rapid exhumation of Eastern Himalaya Syntaxis downstream. We propose that these two co-phased tectonic systems resulting from accelerated extension of southern Tibetan Plateau prevented upstream migration of river knickpoints. Our study highlights that the activity of fault systems may hinder regional erosion, thereby facilitating the preservation of topography and high plateaus in active orogenic belts.

¹Frontiers Science Center for Critical Earth Material Cycling, School of Geography and Ocean Science, Nanjing University, Nanjing 210023, China. ²Key Laboratory of Tibetan Plateau Land Surface Processes and Ecological Conservation (Ministry of Education), Xining 810016, China. ³State Key Laboratory for Mineral Deposits Research, School of Earth Sciences and Engineering, Nanjing University, Nanjing 210023, China. ⁴School of Earth and Ocean Sciences, University of Victoria, Victoria, Canada. ⁵School of Geography, Earth and Atmospheric Sciences, University of Melbourne, Melbourne 3010, Australia. ⁶Laboratory for Mineralogy and Petrology, Department of Geology, Ghent University, Krijgslaan 281, Ghent 9000, Belgium. ✉email: xianyanwang@nju.edu.cn; guangweili@nju.edu.cn

The landscape of an orogenic belt is constantly shaped by competition between tectonic uplift and bedrock river incision¹. It is generally accepted that tectonic uplift increases stream gradient, which conveys more water and sediment via orographic precipitation that facilitates faster incision^{2–5}, driving the headward propagation of river knickpoint^{6–8}. However, why rivers have not incised further or more deeply into active orogenic plateaus to destroy uplifted low-relief terrain over geologic time remains uncertain. The traditional explanation is that pronounced aridity in the interior plateau defeats river incision, and concomitant formation of internally drained basins^{9,10}. Sustained internal drainage and sedimentary infilling of basins^{11,12} reduce elevation contrasts, raising local base levels¹³. In addition, the bidirectional coupling between bedrock river incision and landslides and the resulted drop in landslides frequency through time could lead to a corresponding decrease in the rate of fluvial incision¹⁴. Further, highly local rock uplift^{15,16} or deformation¹⁷, glacier and/or landslide damming^{18–20}, or dynamic feedbacks between tectonics uplift and erosion (i.e. ‘tectonic aneurysm’ model)^{21,22} on the plateau margins have been also viewed as constraining features for the dissection of the plateau morphology by rivers. Thus, the controls on the erosional decay of orogenic plateaus remain controversial.

This debate exists especially in the southern Tibetan Plateau, where is characterized by a relatively low-relief and high-elevation landscape (Fig. 1a, b). The Yarlung River, the largest river in the southern Tibetan Plateau, flows eastward along the Indus-Yarlung Suture zone and then turns southward around the Eastern Himalayan Syntaxis (EHS), creating one of the deepest gorges (Fig. 1b) on Earth^{16,21–23}. Evidence from paleo-altimetry data²⁴ and the sediments in the Himalaya foreland²⁵ and Bengal basins²⁶ show that similar to present-day external drainage systems and high elevation in the southern Tibetan plateau persisted since at least 15 Ma. Meanwhile, the Tibetan plateau since the middle Miocene also underwent active east-west extension²³, resulting in a series of N-S trending rifts developed across the plateau, especially in southern Tibetan Plateau. However, it is uncertain how high elevations in the southern plateau have been sustained in the face of river erosion and fault activity.

Thermochronological ages show a younging trend from the central part of the Tibetan Plateau to the margins (i.e., north-eastern and southeastern margins), suggesting that the plateau may have progressively grown and propagated northeastwards and southeastwards^{27,28}. This expanding uplift has been thought to accelerate river incision from the southeastern margin to the interior plateau^{29–32}, driving the propagation of river knickpoints into the plateau³³. However, some large knickpoints along river valleys coincide in space with local tectonic deformation. For example, knickpoints along the Yarlung River locally coincide with the late Cenozoic N-S trending tectonic rifts (Fig. 1b) that accommodate E-W extension in southern Tibetan Plateau³⁴. This suggests that formation of these knickpoints may have been controlled by active fault-flank uplift. Whether the diverse activity of regional tectonics could have also inhibited knickpoint migration and thus reduced river erosion to maintain topography in southern Tibetan Plateau remains unclear.

To further address this issue, the incision history of the eastern Yarlung River valley in the southern Tibetan Plateau was constrained by low-temperature thermochronology. We collected 23 granite samples along the Gyaca gorge (knickpoint) and the broad valley of the Yarlung River (Supplementary Note 1). A total of 22 apatite fission track (AFT), 6 apatite and 8 zircon (U-Th)/He (AHe and ZHe) ages were obtained (Supplementary Tables 1–3), and previously published thermochronological ages^{33,35,36} in the eastern Yarlung River valley were also compiled

(Fig. 1c, Supplementary Table 4 and Supplementary Fig. 1a). Three-dimensional (3D) thermokinematic modeling was then undertaken to explore the effect of the N-S trending rift on the formation and evolution of the knickpoint and the incision of the Yarlung River. Combined with previous studies, we proposed that fault systems control knickpoints migration and impede river incision in the southern Tibetan Plateau since the late Miocene.

Results

Thermochronological data. New and published thermochronological ages (Supplementary Table 4) along the eastern Yarlung River (from west to east spanning ~330 km) are presented in Fig. 1d (see Supplementary Fig. 1a for further details). Zircon (U-Th)/He (ZHe), apatite fission track (AFT), and apatite (U-Th)/He (AHe) ages range from 23.1 ± 1.4 to 7 ± 1.1 Ma, 17.5 ± 2.6 to 4.2 ± 0.4 Ma, and 9.25 ± 1.49 to 1.75 ± 0.22 Ma, respectively (Supplementary Table 4). The ZHe and AFT ages, except for the relatively young ages in the Gyaca gorge, generally show older ages in the upstream of this gorge compared to those downstream (Fig. 1d). The AHe ages show remarkable youngest ages in the Gyaca gorge and older ages downstream and upstream of this gorge (Fig. 1d).

Thermal history. Cooling histories of the new and previous samples in the study area (divided into 6 Zones, see Fig. 2) were reconstructed using inverse thermal history modelling by the QTQt software³⁷ (Figs. 2a–2f). The spatial and temporal variations of the rock cooling rate since ~12 Ma were calculated from the modeling results (Fig. 2g). The results indicate rapid cooling of the basement rocks in the eastern Yarlung valley between ~12 Ma and ~7 Ma, but the cooling rate has increased obviously in the Gyaca gorge and decreased dramatically in its upstream and downstream since ~7 Ma (Fig. 2g).

3D thermo-kinematic modeling. To further explore possible mechanisms governing the regional erosion history, 3D thermokinematic modeling strategy using Pecube was applied (detailed setting of the models described in Supplementary Table 5). We constructed two scenarios, i.e. one without (Scenario A), and then with the influence of the Woca fault that bounds the rift structure (Scenario B) (Supplementary Fig. 2). Based on our thermal history modeling results above, the first model (Scenario A) was set-up with a two-stage (12–7 Ma and 7–0 Ma) evolution history without Woca fault activity. More than 20,000 iterations were run to find the best fitting model that constrains the incision rate of the Yarlung River. The best-fitting results exhibit a first stage of rapid incision rates of 1.98 km Ma^{-1} , followed by a second stage with a decreased rate of 0.45 km Ma^{-1} (Supplementary Table 6 and Supplementary Fig. 3). The model predicted thermochronological ages, which are generally consistent with those actually observed for samples located > 25 km away from the Gyaca gorge. However, for those samples located nearby the Gyaca gorge (in the footwall of the Woca fault), the predicted AFT and AHe ages are much older than those measured (Fig. 3a, e). These large differences suggest that Scenario A, which did not integrate normal fault movements, was unable to fit the spatial distribution of observed AHe and AFT ages (Fig. 3a, e).

For Scenario B, we added a normal fault to simulate a more complex uplift velocity field. Based on our thermal history modeling results, the time of initial normal fault activity was set at 7 Ma (Fig. 2g), and the fault trace at the surface follows that of the Woca fault (see Fig. 1c). Due to the lack of geophysical data constraining the deeper sections of the fault, we ran three distinct inversions in which we fixed the deepest segment to be horizontal at depths of 20, 30, and 50 km, respectively. The results show that

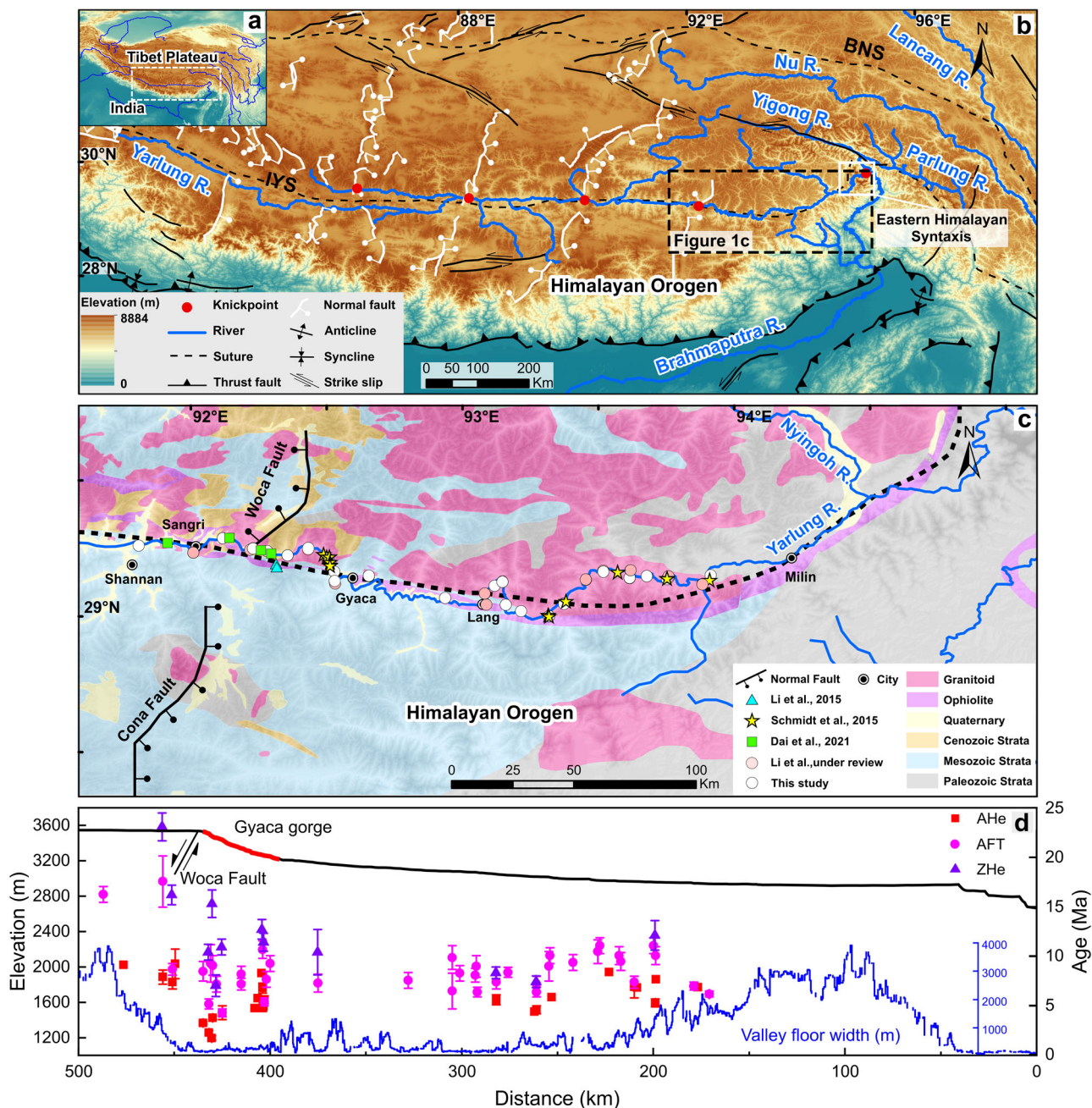


Fig. 1 Regional background. **a** Topography of the Tibetan Plateau and its major rivers. **b** Major faults, rivers and topography of the southern Tibetan Plateau. The red dots represent large knickpoints in the Yarlung River. Dashed rectangle shows the extent of Fig. 1c. The white square shows the location of the Eastern Himalayan Syntaxis. BNS, Bangong-Nujiang Suture zone; IYS, Indus-Yarlung Suture zone. **c** Simplified geological map⁷⁶ and sample locations along the eastern Yarlung River. **d** New and published thermochronological ages^{33,35,36} (Supplementary Table 4) along the eastern Yarlung River. AHe, apatite (U-Th-Sm)/He; AFT, apatite fission track; ZHe, zircon (U-Th)/He. Vertical error bars indicate 1 σ uncertainty for thermochronological ages. The black and blue lines represent river profile and valley floor width, respectively. The river profile was extracted from ~30 m Shuttle Radar Topography Mission (SRTM) digital elevation model data, smoothing profiles used a LOESS filter to decrease noise and highlight the general shape of the river profile. The valley floor width was measured from Google Earth Image (Supplementary Note 1 and Supplementary Fig. 9).

the three models for Scenario B successfully reproduced the AHe and AFT ages in the Gyaca gorge (Fig. 3b–d, f–h), and that the spatial distribution of predicted ages is generally consistent with measured ages (Figs. 3b–d, f–h). This confirms that incision of the eastern Yarlung River was indeed strongly influenced by a normal fault since ~7 Ma.

Comparing the misfit values of the inversion for the three models in scenario B (Fig. 3f–h, Supplementary Table 6), we found that values for the model coupled with a 30 (3.92) or

50 km-depth fault (4.07) seem a little lower than that for a 20 km-depth fault (4.17). This would indicate that the depth of the Woca fault could reach up to ~30 km or more. Furthermore, these models predict a steep (68°~75°) fault in the shallow crust, near the surface (Fig. 3c, d), and a fault-slip velocity rate of $1.19 \pm 0.03 \text{ km Ma}^{-1}$ since 7 Ma (Supplementary Table 6 and Supplementary Figs. 4–6). This finding is in very good agreement with the observed high-angle fault geometry of 60°~75°³⁸ and the Quaternary slip rate of $1.2 \pm 0.6 \text{ km Ma}^{-1}$ ¹³⁹. The model also

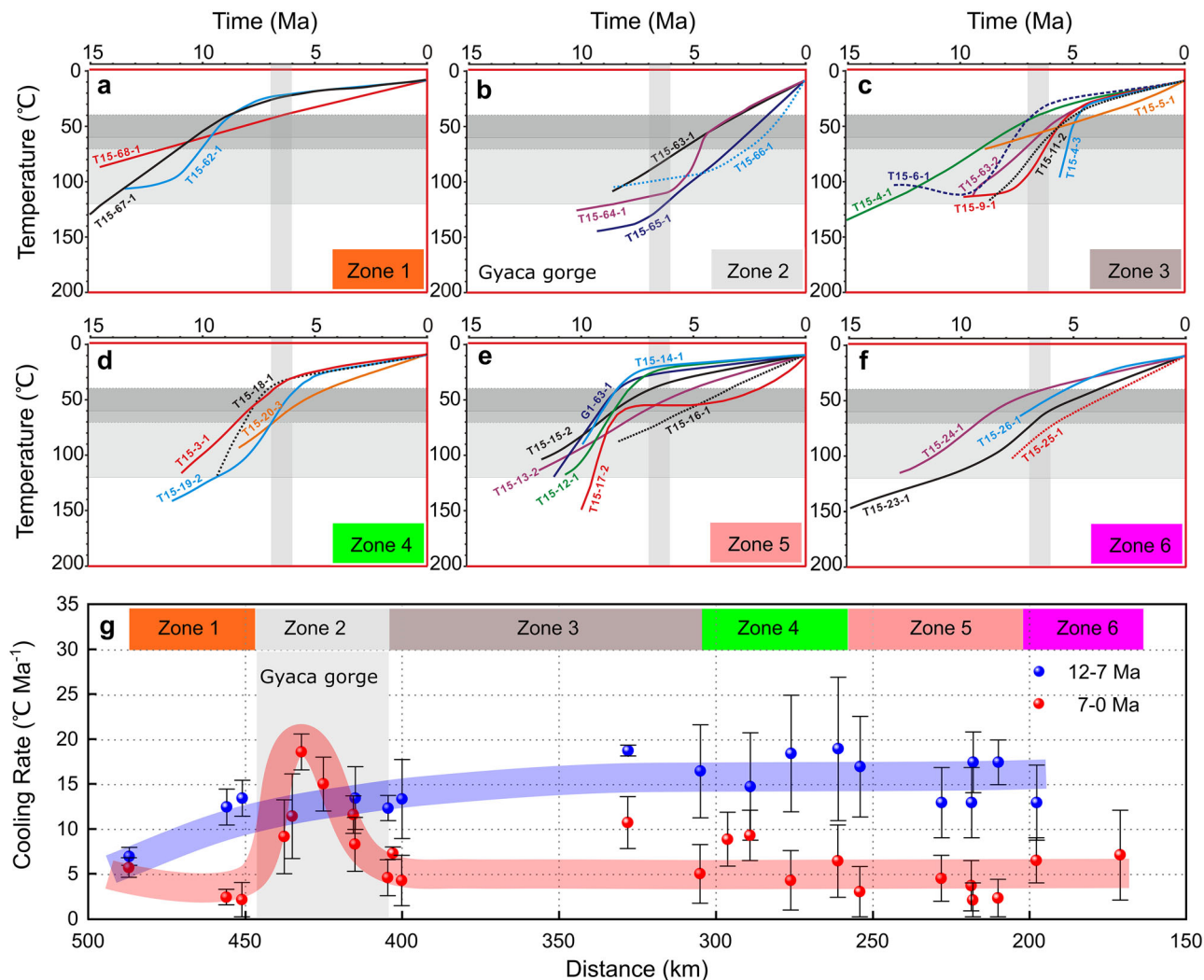


Fig. 2 Inverse thermal history models from QTQt based on available thermochronological data (Supplementary Table 4) along the eastern Yarlung River. **a–f** Cooling histories of bedrock samples from west to east along the Yarlung River. Zone 1, upstream of the Gyaca gorge (hanging wall of the Woca normal fault); Zone 2, the Gyaca gorge (footwall of the Woca normal fault); Zone 3–6, downstream of the Gyaca gorge. Different colored lines indicate best-fit modelled thermal paths for different samples. **g** Spatial and temporal pattern of cooling rates calculated from thermal history modeling results. Black error bars denote the standard deviation using three different cooling rates (see Supplementary Note 4 for further details).

shows that the incision rate along the eastern Yarlung River was up to $1.73 \pm 0.07 \text{ km Ma}^{-1}$ between 12 Ma and 7 Ma, followed by a rather slow incision rate of $0.18 \pm 0.03 \text{ km Ma}^{-1}$ upstream and downstream of the Gyaca gorge since 7 Ma (Supplementary Table 6 and Supplementary Figs. 4–6). This is also broadly consistent with the thermochronology results.

Discussion

Fault activity controls the formation of knickpoint. In a previous study³³, Schmidt et al. proposed that the Gyaca knickpoint resulted from upstream migration of erosional waves starting from the Yarlung Tsangpo Grand Canyon (Fig. 1b) in response to uplift of the southeastern Tibetan Plateau prior to $\sim 10 \text{ Ma}$ ³³. However, no geomorphic evidence (e.g., terraces) for downstream knickpoint retreat has been reported, although the decrease of base level at the Yarlung Tsangpo Grand Canyon might result in fluvial incision³³. Our modeling results suggest that both headward incision of the Yarlung River since $\sim 12 \text{ Ma}$ due to uplift of the southeastern Tibetan Plateau³³ or intensified monsoon precipitation^{40,41} are not compatible with the remarkable young AHe and AFT ages in the Gyaca gorge (Fig. 3e). In addition, rock

outcrops in the Gyaca gorge and its downstream valley are mainly granitoids (Fig. 1c), thus lithological variation cannot be attributed as a major controlling factor for the formation of the Gyaca gorge. In contrast, as indicated by the well constrained Pecube model, a high-angle normal fault is required (Scenario B), to fit with an increased rock cooling rate at the Gyaca gorge since $\sim 7 \text{ Ma}$ (Fig. 3g). Therefore, we argue that movement of the Woca fault has controlled the formation of the Gyaca knickpoint since $\sim 7 \text{ Ma}$, and that a similar mechanism might also explain the formation of other large knickpoints in the middle and upper reaches of the Yarlung River (Fig. 1b).

Based on QTQt and Pecube modeling results, a relatively high incision rate ($\sim 1.73 \pm 0.07 \text{ km Ma}^{-1}$) of the eastern Yarlung River initiated at $\sim 12 \text{ Ma}$, with a slightly decreasing trend in thermochronological ages from west to east along the Yarlung River. Published thermochronometric data from the externally drained portion of the eastern^{15,42,43} and central^{44,45} Lhasa terrane, as well as from large rivers in the southeastern Tibetan Plateau^{41,46}, demonstrate that rapid exhumation rates ($> 1 \text{ km Ma}^{-1}$) were pervasive across the southern and southeastern plateau between ~ 17 and 10 Ma . These spatially large-scale synchronous rapid incision events most likely reflect

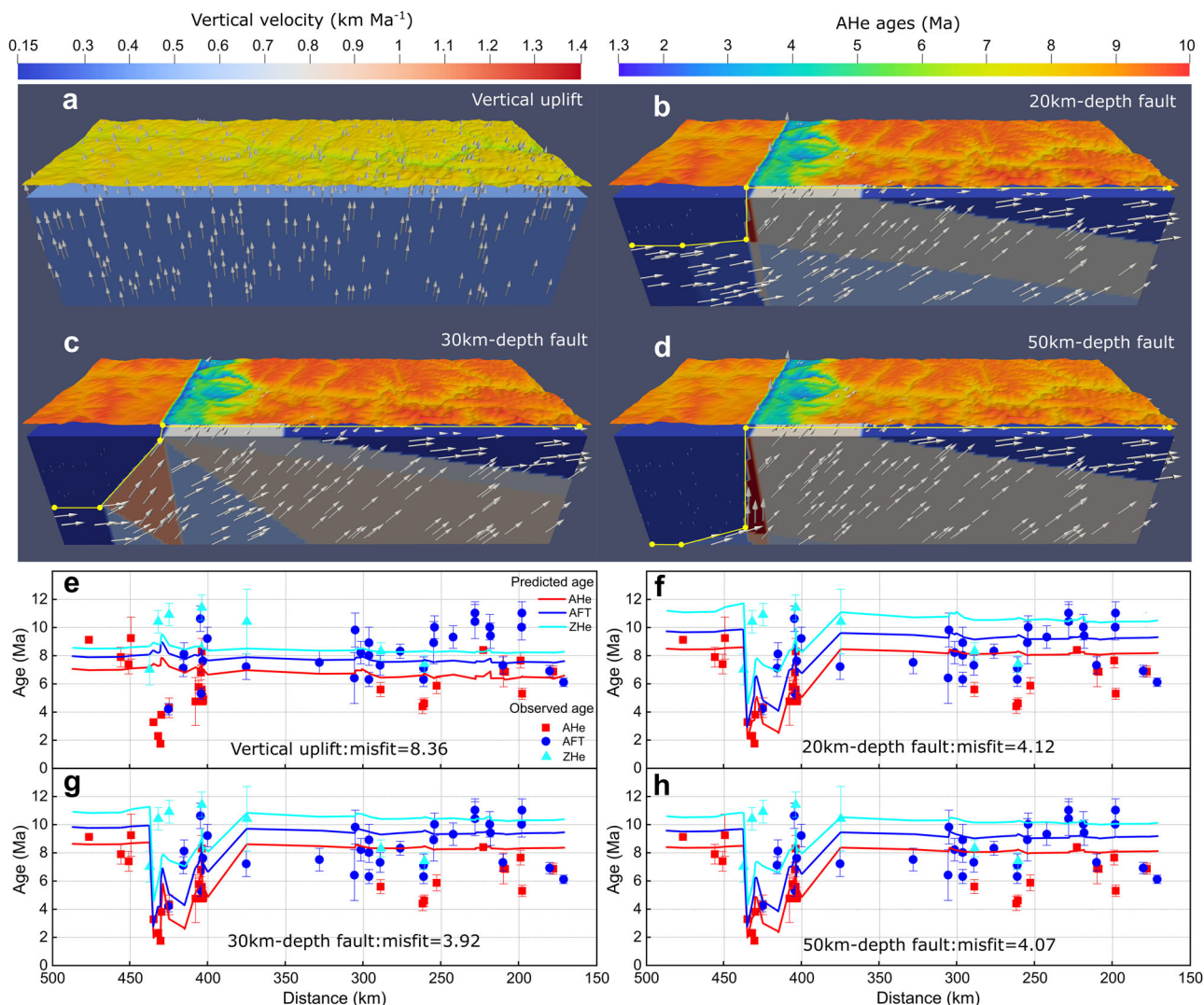


Fig. 3 Results of thermo-kinematic inversion and forward modeling. **a–d** The vertical velocity of thermo-kinematic inversion during the recent exhumation phase (7–0 Ma) and the predicted AHe ages for different scenarios. The arrows reflect the direction of movement of rock particles with **(a)** and without a normal fault **(b, c, d)**. The yellow dots represent inflection points defining fault geometry. **e–h** Comparison between observed and predicted cooling ages along the eastern Yarlung River from the corresponding forward modeling of different scenarios since 12 Ma. Vertical error bars indicate 1σ uncertainty for observed age.

enhanced Asian summer monsoon precipitation in the mid-Miocene^{40,41} that promoted the headward erosion of the Yarlung River channels (Fig. 4a). However, the incision rate upstream and downstream of the Gyaca gorge has decreased dramatically with the rapid activity of the Woca fault since 7 Ma (Fig. 2g and Supplementary Table 6).

Onset of EHS exhumation and its link to rifting. Thermo-chronometric data from rifts in the Tibetan Plateau^{47,48} suggest that southern Tibetan Plateau has experienced rapid late Miocene to Pliocene rift acceleration³⁴ (see Supplementary Fig. 7). This rapid rift activity with accelerated extension of southern Tibetan Plateau controls knickpoints, such as the Gyaca knickpoint, in the plateau interior. Further, the high rate of rifts extension in southern Tibetan Plateau also facilitate thinning of the upper crust while its lower crust is thickened by ongoing compression^{34,49,50}. This could contribute to accelerating eastward crustal flow⁵¹ at the Eastern Himalayan Syntaxis (EHS) driving localized deformation and uplift^{52–54}, leading to active coupling between crustal rock advection and river erosion⁵⁵ since ~7 Ma (Fig. 4b). Detrital thermo-chronological data from foreland basin sediments downstream of

the EHS also suggest coupling between tectonic uplift and erosion starting at 8 Ma⁵⁵, 7–5 Ma⁵⁶ and/or 6–4 Ma⁵⁷.

Currently, the mechanism of rapid exhumation in the EHS remains controversial. A current paradigm is the Tectonic Aneurysm model, in which spatially focused surface erosion driven by the Yarlung River locally might accelerate rock uplift and exhumation of hot and weak crust at the syntaxes^{21,22,58}. Evidence from sediments in the Himalaya foreland²⁵, Bengal basins²⁶ and our thermochronometric data (Fig. 2) show that the Yarlung River was definitely set in its course before ~12 Ma. However, this does not specifically address the role of the Yarlung River in driving initial rapid exhumation of the EHS, which is thought to have begun 8–6 Ma^{55–57}. Although Wang et al. argued for a rapid uplift of the EHS at ~2.5 Ma based on sediment fill immediately upstream of the Yarlung Zangbo gorge^{16,59,60}, we consider this as only one of several stages of EHS uplift, rather than the initial uplift episode. The work by King et al. shows that the optically stimulated luminescence thermochronology to the northeast of the Namche Barwa supports the idea of northward migration of the high exhumation locus (as proposed by Seward and Burg⁶¹) instead of control by localized very fast fluvial incision⁶². Here, we find evidence for a synchronous exhumation pulse in the rifts

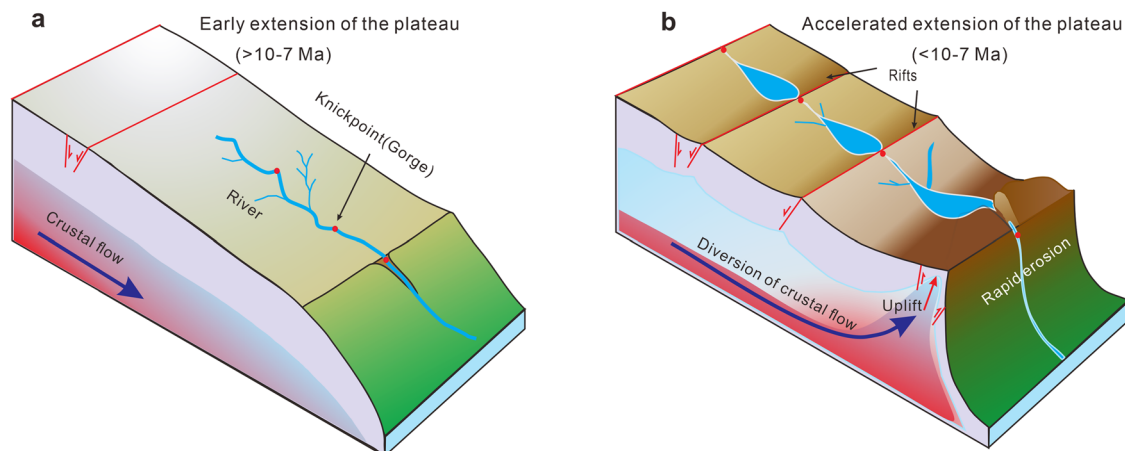


Fig. 4 Schematic diagram illustrating the mechanisms for tectonic activity impeding the river incision. a Headwater incision of the river related to the uplift of the southeastern Tibetan Plateau along with intensified monsoon precipitation. **b** Regional coupled tectonic systems with accelerated extension of the plateau driving the formation of river knickpoints, which subsequently adjusts and reduces the regional river gradient, keeping river knickpoints relatively stable and slowing down upstream river incision.

(Supplementary Fig. 7) and EHS⁵⁵ since the late Miocene. This rapid exhumation implies that the tectonic system resulting from the accelerated late Miocene extension of southern Tibetan Plateau drove regional fault activity to control rapid exhumation and the formation of stable knickpoints in the rifts and EHS.

Contribution of stable knickpoints to the stabilization of southern Tibetan Plateau. With the stabilization of knickpoints, the landscape equilibrates towards topographic steady-state equilibrium whereby for a given climatic condition, the slope of rivers adjust toward a geometry that allows an incision rate equal to rock uplift rate⁶³. Therefore, the surface uplift rate might be zero, which would sustain a high-elevation base level for the Yarlung River in the rifts and EHS. Meanwhile, coeval tectonic evolution with the accelerated late Miocene extension of southern Tibetan Plateau contribute to the stabilization of southern Tibetan Plateau. If only local fault activity of the rift controlled the Gyaca knickpoint (Fig. 1b, c), and the localized deformation and uplift of EHS downstream were not particularly fast, so that EHS knickpoint was not fixed (Fig. 1b), it would migrate headwards, gradually towards the Gyaca gorge. This would cause the base level to fall in the region and the river would incise more deeply into the plateau interior.

With the stabilization of the knickpoints, river gradients above the knickpoints are commonly so low that fluvial incision may generally have difficulty in keeping up with increase in tectonic uplift rates. As a result, channel slope and stream power would decrease transiently above these Yarlung River knickpoints (Fig. 4b). Simultaneously, the reduced river gradient and sediment flux could promote upstream aggradation, burial of bedrock valley floors^{19,64,65}, and valley widening (Fig. 1d, b), which could cause widespread backwater aggradation, forming broad valley trains occupied today by braided river systems (Fig. 1d and Supplementary Fig. 1b–f). Field survey also found large paleo-lakes⁶⁶ upstream and valley-fill sediments¹⁶ downstream of Gyaca gorge (Supplementary Fig. 8). This braided river only incised when the stripping of deposited alluvial material exposed bedrock to processes of abrasion, weathering and plucking⁶⁷. Therefore, the erosion rate of the river above the knickpoints will be reduced obviously due to the reduction of stream power since the late Miocene. This is supported by the predicted low erosion rates ($0.18 \pm 0.03 \text{ km Ma}^{-1}$) (Supplementary Table 6 and Supplementary Figs. 4–6), which is in agreement

with the rates ($0.04\text{--}0.20 \text{ km Ma}^{-1}$) determined from cosmogenic nuclide (^{10}Be) data in the middle reaches of the Yarlung River⁶⁸.

Hence, coeval tectonic systems (rifting upstream and uplift and exhumation of the EHS downstream) with the accelerated extension of southern Tibetan Plateau resulted not only in upstream reduction in river gradient and stream power, but also stabilized downstream base levels, i.e. from a stable knickpoint at the EHS. This would subsequently drive the onset of stable knickpoints formation in the Gyaca and EHS, thereby impeding a wave of upstream erosion and facilitating the stabilization of southern Tibetan Plateau topography since the late Miocene.

Processes controlling the stability/instability of knickpoints in active orogens.

When uplift rates are spatially variable for a given climatic condition, two fundamentally distinctive types of knickpoints (i.e. transient and stationary knickpoints) might develop under different conditions^{3,4,69}. Transient knickpoints, which may be produced by a change in the background regional uplift rate or a discrete base-level lowering event⁶⁹. Whereas stationary knickpoints may reflect abrupt spatial changes in uplift/incision rate⁶⁹, and/or a hard basement³. Based on our results (Fig. 4) and published literature⁶⁹, we suggest that the transient migration and stability of river knickpoints might coexist during the evolution of orogenic belts. For example, many other active orogenic belts also first grow to a certain height, and then experience laterally outward propagation⁷⁰. This expanding uplift generally increases the steepness of rivers, and promotes upstream erosion^{30–32}. But this expansion is not a simple one-dimensional process, it might also be accompanied by diverse strong regional tectonic deformation of the upper crust^{17,71,72} (e.g., rifting, subduction, and strike-slip faulting) and lower crustal flow⁵¹. Lower crustal flow in turn will promote and further drive regional tectonic deformation of the upper crust, leading to the stability of knickpoints. An excellent example of channel adjustment to tectonic forcing is the Eastern-Western Himalaya Syntaxis^{52,53}. However, clearly not all knickpoints associated with active faulting are stalled, such as the locations of the Hatay Graben in Turkey⁷³, a normal fault system in the eastern California³ and the headwaters of the Yellow River in the Tibetan Plateau⁷⁴, which might be mainly related to the dip and slip rate of faults^{73,74}. The Woca normal fault in this study is dipping in the upstream direction (Fig. 1c), which might reduce the amount of base-level fall experienced by that part of the Tibetan Plateau which is drained by the Yarlung River. Thus, we propose that the

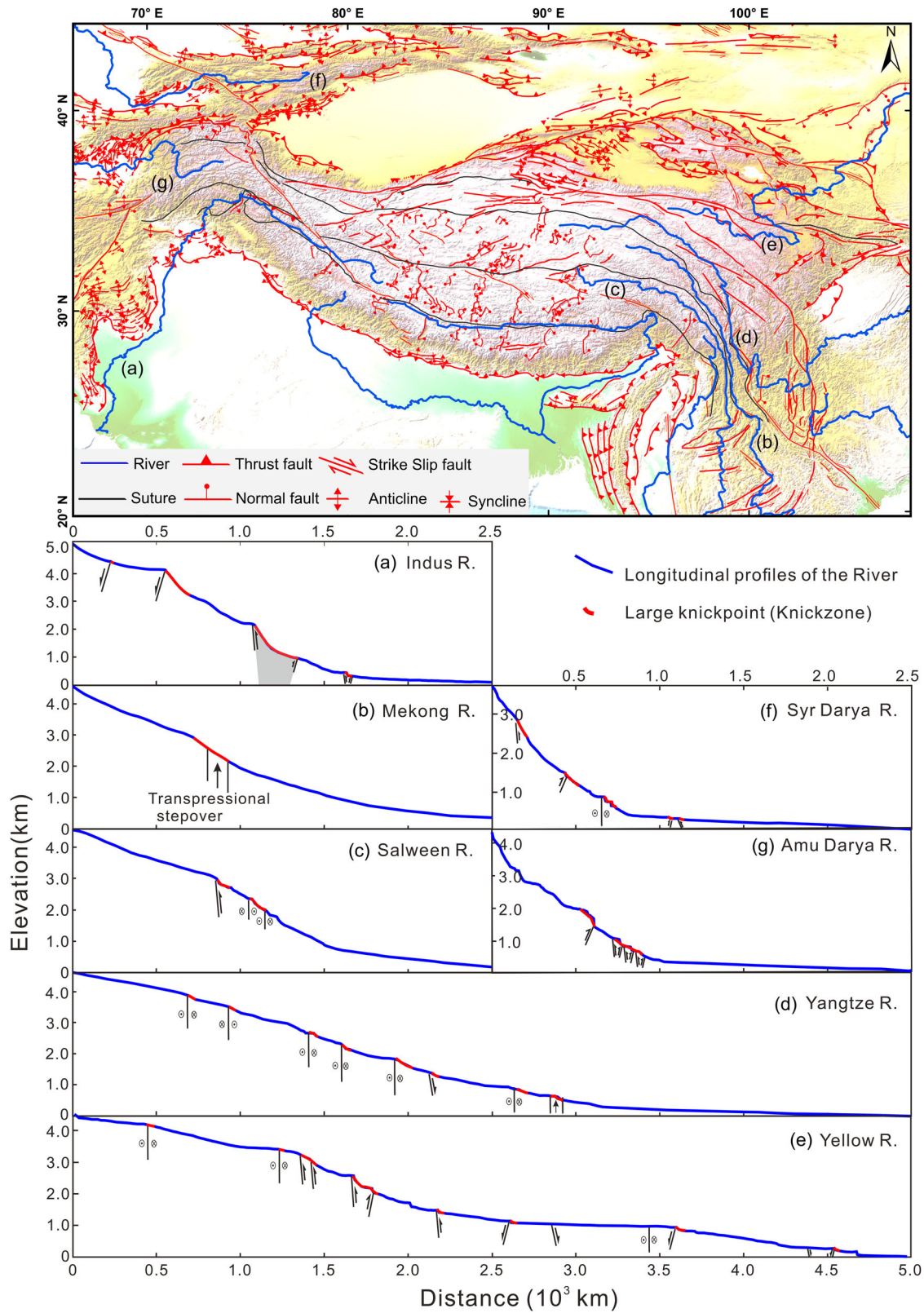


Fig. 5 Spatial distribution of regional tectonic features and large knickpoints along major rivers in the Tibetan Plateau. **a** Longitudinal profiles of Indus River. **b** Mekong River. **c** Salween River. **d** Yangtze River. **e** Yellow River. **f** Syr Darya River. **g** Amu Darya River.

activity of the local fault systems can limit the migration of these river knickpoints under specific conditions, such as those on the eastern Yarlung River, which are still located in the area of regional tectonic deformation (Fig. 5). This process should

subsequently reduce fluvial incision in the upstream and prevent base-level fall downstream of the knickpoints. This might stabilize the topography of the Plateau and protect high-elevation, low-relief surfaces over geologic time in active orogenic belts.

Our findings suggest that tectonic activity does not always necessarily enhance fluvial incision, and that the diverse activity can also decrease these rates by the adjustment of fault systems in active orogenic belts. This finding also provides a new mechanism for explaining the universal stability of topography and high plateaus in some other orogenic belts.

Methods

Thermochronological data and thermal history. Apatite and zircon separates were concentrated using standard heavy liquid and magnetic separation techniques. Analyses were performed at the School of Geography, Earth and Atmospheric Sciences, University of Melbourne (see Supplementary Note 2, 3 for further details). The thermal histories based on these thermochronological data were determined using the QTQt software³⁷ (details in Supplementary Note 4), and spatial and temporal cooling pattern and rates along the Yarlung River were calculated based on the model results.

3D thermo-kinematic modeling. To identify detailed effects of rift activity on Yarlung River incision, we used the thermokinematic finite-element Pecube⁷⁵ code, which has been developed to interpret thermochronological data by solving a 3D crustal heat-transport equation. We constructed two scenarios in Pecube, i.e. without (Scenario A) and with the influences of the Woca fault (Scenario B) (detailed model parameters are described in Supplementary Note 5). In Scenario A, the Yarlung River was incised from a flat plateau surface to form the topography, ignoring the influence of the Woca normal fault in the plateau interior. This scenario mainly reflects the upstream migration of erosional waves of the Yarlung River (Supplementary Fig. 2). In Scenario B, we considered not only the incision of the Yarlung River, but also incorporated the effect of the Woca normal fault (see Supplementary Fig. 2).

Data availability

All thermochronological data used in this study are available in <https://figshare.com/s/4aa78f1a9ebd4c7105a2>. Results of thermal history models from QTQt and 3D thermo-kinematic inversion in this study have been deposited in the Figshare Data Repository, respectively. (<https://figshare.com/articles/figure/QTQt/22110746>); (<https://figshare.com/s/dd1203e7834449827c74>). Topographic and faults data in Figs. 1 and 5 are obtained from the open-source databases (<https://www.ngdc.noaa.gov/mgg/topo/> and <https://github.com/HimaTibetMap/HimaTibetMap>).

Code availability

The code Pecube, used in this work, is open source and can be downloaded at <https://github.com/jeanbraun/Pecube>.

Received: 3 November 2022; Accepted: 22 May 2023;

Published online: 05 June 2023

References

- England, P. & Molnar, P. Surface uplift, uplift of rocks, and exhumation of rocks. *Geology* **19**, 1051–1053 (1991).
- Clark, M. et al. Surface uplift, tectonics, and erosion of Eastern Tibet from large-scale drainage patterns. *Tectonics* **23**, TC1006 (2004).
- Kirby, E. & Whipple, K. Expression of active tectonics in erosional landscapes. *J. Struct. Geol.* **44**, 54–75 (2012).
- Whipple, K. Bedrock rivers and the geomorphology of active orogens. *Annu. Rev. Earth Planet. Sci.* **32**, 151 (2004).
- Lease, R. & Ehlers, T. Incision into the eastern Andean Plateau during Pliocene cooling. *Science (New York, NY)* **341**, 774–776 (2013).
- Schildgen, T. F., Balco, G. & Shuster, D. L. Canyon incision and knickpoint propagation recorded by apatite He^4/He^3 thermochronometry. *Earth Planet. Sci. Lett.* **293**, 377–387 (2010).
- Yang, R. et al. Spatial and temporal pattern of erosion in the three rivers region, southeastern Tibet. *Earth Planet. Sci. Lett.* **433**, 10–20 (2016).
- Willett, S., McCoy, S., Perron, J., Goren, L. & Chen, C. Y. Dynamic reorganization of river Basins. *Science (New York, NY)* **343**, 1117 (2014).
- Sobel, E., Hilley, G. & Strecker, M. Formation of internally drained contractional basins by aridity-limited bedrock incision. *J. Geophys. Res.: Atmos.* **108**, 1–6 (2003).
- Garcia-Castellanos, D. The role of climate during high plateau formation. Insights from numerical experiments. *Earth Planet. Sci. Lett.* **257**, 3–4 (2007).
- Heidarzadeh, G., Ballato, P., Hassanzadeh, J., Ghassemi, M. & Strecker, M. Lake overflow and onset of fluvial incision in the Iranian Plateau: Insights from the Mianeh Basin. *Earth Planet. Sci. Lett.* **469**, 135–147 (2017).
- House, P., Pearthree, P. & Perkins, M. Stratigraphic evidence for the role of lake spillover in the inception of the lower Colorado River in southern Nevada and western Arizona. *Spec. Pap. Geol. Soc. Am.* **439**, 335–353 (2008).
- Pingel, H., Alonso, R., Altenberger, U., Cottle, J. & Strecker, M. Miocene to Quaternary basin evolution at the southeastern Andean Plateau (Puna) margin (~24°S lat, Northwestern Argentina). *Basin Res.* **31**, 808–826 (2019).
- Egholm, D. L., Knudsen, M. F. & Sandiford, M. Lifespan of mountain ranges scaled by feedbacks between landsliding and erosion by rivers. *Nature* **498**, 475–478 (2013).
- Tremblay, M. M. et al. Erosion in southern Tibet shut down at ~ 10 Ma due to enhanced rock uplift within the Himalaya. *Proc. Natl. Acad. Sci. USA* **112**, 12030–12035 (2015).
- Wang, P. et al. Tectonic control of Yarlung Tsangpo Gorge revealed by a buried canyon in Southern Tibet. *Science* **346**, 978–981 (2014).
- Seagren, E. & Schoenbohm, L. Drainage Reorganization Across the Puna Plateau Margin (NW Argentina): Implications for the Preservation of Orogenic Plateaus. *J. Geophys. Res.* **126**, 1–28 (2021).
- Korup, O. & Montgomery, D. Tibetan plateau river incision inhibited by glacial stabilization of the Tsangpo gorge. *Nature* **455**, 786–789 (2008).
- Korup, O., Montgomery, D. & Hewitt, K. Glacier and landslide feedbacks to topographic relief in the Himalayan syntaxes. *Proc. Natl. Acad. Sci. USA* **107**, 5317–5322 (2010).
- Owen, L. Geomorphology: How Tibet might keep its edge. *Nature* **455**, 748–749 (2008).
- Zeitler, P. et al. Erosion, Himalayan geodynamics, and the geomorphology of metamorphism. *GSA Today* **11**, 4–9 (2001).
- Koons, P. O., Zeitler, P., & Hallet, B. Tectonic Aneurysms and Mountain Building, in *Treatise on Geomorphology*, John F. Shroder, Ed. (Academic Press, San Diego), pp. 318–349. 2013.
- Yin, A. & Harrison, T. M. Geologic evolution of the Himalayan-Tibetan orogen. *Annu. Rev. Earth Planet. Sci.* **28**, 211–280 (2000).
- Spicer, R. et al. Constant elevation of southern Tibet over the past 15 million years. *Nature* **421**, 622–624 (2003).
- Lang, K. & Huntington, K. Antecedence of the Yarlung–Siang–Brahmaputra River, eastern Himalaya. *Earth Planet. Sci. Lett.* **397**, 145–158 (2014).
- Bracciali, L., Najman, Y., Parrish, R., Akhter, S. & Millar, I. The Brahmaputra tale of tectonics and erosion: Early Miocene river capture in the Eastern Himalaya. *Earth Planet. Sci. Lett.* **415**, 25–37 (2015).
- Li, Y. L. et al. Propagation of the deformation and growth of the Tibetan-Himalayan orogen: A review. *Earth Sci. Rev.* **143**, 36–61 (2015).
- Li, H. A. et al. The formation and expansion of the eastern Proto-Tibetan Plateau: Insights from low-temperature thermochronology. *J. Asian Earth Sci.* **183**, 103975 (2019).
- Clark, M. et al. Late Cenozoic uplift Southeastern Tibet. *Geology* **33**, 525–528 (2005).
- Harkins, N., Kirby, E., Heimsath, A., Robinson, R. & Reiser, U. Transient Fluvial Incision in the Headwaters of the Yellow River, Northeastern Tibet, China. *J. Geophys. Res.* **112**, 3–4 (2007).
- Ouimet, W. et al. Regional incision of the eastern margin of the Tibetan Plateau. *Lithosphere* **2**, 50–63 (2010).
- Yuan, X. et al. Propagating uplift controls on high-elevation, low-relief landscape formation in the southeast Tibetan Plateau. *Geology* **50**, 60–65 (2021).
- Schmidt, J. et al. Knickpoint evolution on the Yarlung river: Evidence for late Cenozoic uplift of the southeastern Tibetan plateau margin. *Earth Planet. Sci. Lett.* **430**, 448–457 (2015).
- Styron, R., Taylor, M. & Sundell, K. Accelerated extension of Tibet linked to the northward underthrusting of Indian crust. *Nat. Geosci.* **8**, 131–134 (2015).
- Dai, J. G. et al. Two stages of accelerated exhumation in the middle reach of the Yarlung River, Southern Tibet since the mid-Miocene. *Tectonics* **40**, 1–17 (2021).
- Li, G. et al. Cenozoic low temperature cooling history of the Northern Tethyan Himalaya in Zedang, SE Tibet and its implications. *Tectonophysics* **643**, 80–93 (2015).
- Gallagher, K. Transdimensional inverse thermal history modeling for quantitative thermochronology. *J. Geophys. Res.: Solid Earth* **117**, 1–16 (2012).
- Wu, Z., Zhang, Y., Hu, D. & Zhao, X. Late Cenozoic normal faulting of the Qungdogyang graben in the central segment of the Cona-Oiga rift, Southeastern Tibet. *Journal of Geomechanics* **13**, 297–306 (2007).
- Wu, Z., Zhang, Y., Hu, D. G., Zhao, X. & Ye, P. S. The Quaternary normal faulting of the Cona-Oiga rift. *Seismology and Geology* **30**, 144–160 (2008).
- Clift, P. D. et al. Correlation of Himalayan exhumation rates and Asian monsoon intensity. *Nat. Geosci.* **1**, 875–880 (2008).
- Nie, J. S. et al. Rapid incision of the Mekong River in the middle Miocene linked to monsoonal precipitation. *Nat. Geosci.* **11**, 944–948 (2018).

42. Copeland, P. et al. Thermal evolution of the Gangdese batholith, southern Tibet: A history of episodic unroofing. *Tectonics* **14**, 223–236 (1995).
43. Li, G. W. et al. Synorogenic morphotectonic evolution of the Gangdese batholith, South Tibet: Insights from low-temperature thermochronology. *Geochem., Geophys., Geosyst.* **17**, 101–112 (2016).
44. Carrapa, B. et al. Miocene burial and exhumation of the India-Asia collision zone in southern Tibet: Response to slab dynamics and erosion. *Geology* **42**, 443–446 (2014).
45. Su, W. et al. Late Oligocene - Miocene morpho-tectonic evolution of the central Gangdese batholith constrained by low-temperature thermochronology. *Tectonophysics* **840**, 229559 (2022).
46. Cai, D., Wang, X., Li, G., Zhu, W. & Lu, H. Late Cenozoic denudation and topographic evolution history of the Lhasa River drainage in southern Tibetan Plateau: insights from inverse thermal history modeling. *Front. Earth Sci.* **9**, 636459 (2022).
47. Bian, S. et al. Late Pliocene onset of the Cona rift, eastern Himalaya, confirms eastward propagation of extension in Himalayan-Tibetan orogen. *Earth Planet. Sci. Lett.* **544**, 116383 (2020).
48. Lee, J. et al. Middle to late Miocene extremely rapid exhumation and thermal reequilibration in the Kung Co rift, southern Tibet. *Tectonics* **30**, 1–26 (2011).
49. McDermott, J., Whipple, K., Hodges, K. & van Soest, M. Evidence for Plio-Pleistocene north-south extension at the southern margin of the Tibetan Plateau, Nyalam region. *Tectonics* **32**, 317–333 (2013).
50. Sundell, K. et al. Evidence for constriction and Pliocene acceleration of east-west extension in the North Lunggar rift region of west central Tibet. *Tectonics* **32**, 1454–1479 (2013).
51. Clark, M. & Royden, L. Topographic ooze: Building the eastern margin of Tibet by lower crustal flow. *Geology* **28**, 703–706 (2000).
52. Whipp, D., Beaumont, C. & Braun, J. Feeding the “aneurysm”: Orogen-parallel mass transport into Nanga Parbat and the western Himalayan syntaxis. *J. Geophys. Res.: Solid Earth* **119**, 5077–5096 (2014).
53. Ding, L., Zhong, D., Yin, A., Kapp, P. & Harrison, T. M. Cenozoic structural and metamorphic evolution of the eastern Himalayan syntaxis (Namche Barwa). *Earth Planet. Sci. Lett.* **192**, 423–438 (2001).
54. Guevara, V. et al. A modern pulse of ultrafast exhumation and diachronous crustal melting in the Nanga Parbat Massif. *Science Advances* **8**, eabm2689 (2022).
55. Govin, G. et al. Early onset and late acceleration of rapid exhumation in the Namche Barwa syntaxis, eastern Himalaya. *Geology* **48**, 1139–1143 (2020).
56. Lang, K., Huntington, K., Burmester, R. & Housen, B. Rapid exhumation of the eastern Himalayan syntaxis since the late Miocene. *Geol. Soc. Am. Bull.* **128**, 1403–1422 (2016).
57. Najman, Y. et al. Spatial and temporal trends in exhumation of the Eastern Himalaya and syntaxis as determined from a multitechnique detrital thermochronological study of the Bengal Fan. *Geol. Soc. Am. Bull.* **131**, 1607–1622 (2019).
58. Hodges, K. & Whipple, K. Dynamic processes at the ends of collisional mountain chains. *Science advances* **8**, eade6607 (2022).
59. Zeitler, P., Koons, P., Hallet, B. & Meltzer, A. Geomorphology. Comment on “Tectonic control of Yarlung Tsangpo Gorge revealed by a buried canyon in Southern Tibet”. *Science (New York, NY)* **349**, 799 (2015).
60. Wang, P. et al. Response to Comment on “Tectonic control of Yarlung Tsangpo Gorge revealed by a buried canyon in Southern Tibet”. *Science* **349**, 799 (2015).
61. Seward, D. & Burg, J. P. Growth of the Namche Barwa Syntaxis and associated evolution of the Tsangpo Gorge: Constraints from structural and thermochronological data. *Tectonophysics* **451**, 282–289 (2008).
62. King, G., Herman, F. & Guralnik, B. Northward migration of the eastern Himalayan syntaxis revealed by OSL thermochronometry. *Science* **353**, 800–804 (2016).
63. Tejedor, A., Singh, A., Zaliapin, I., Densmore, A. & Fofoula-Georgiou, E. Scale-dependent erosional patterns in steady-state and transient-state landscapes. *Science Advances* **3**, e1701683 (2017).
64. Humphrey, N. & Konrad, S. River incision or diversion in response to bedrock uplift. *Geology* **28**, 43–46 (2000).
65. Hilley, G. & Strecker, M. Processes of oscillatory basin filling and excavation in a tectonically active orogen: Quebrada Del Toro Basin, NW Argentina. *Geol. Soc. Am. Bull.* **117**, 887–901 (2005).
66. Zhu, S., Wu, Z. H., Zhao, X. T. & Xiao, K. Y. Glacial dammed lakes in the Tsangpo River during late Pleistocene, southeastern Tibet. *Quat. Int.* **298**, 114–122 (2013).
67. Finnegan, N., Schumer, R. & Finnegan, S. A signature of transience in bedrock river incision rates over timescales of 104–107 years. *Nature* **505**, 391–394 (2014).
68. Lupker, M. et al. ¹⁰Be systematics in the Tsangpo-Brahmaputra catchment: the cosmogenic nuclide legacy of the eastern Himalayan syntaxis. *Earth Surf. Dynam.* **5**, 429–449 (2017).
69. Royden, L. & Perron, J. Solutions of the stream power equation and application to the evolution of river longitudinal profiles. *J. Geophys. Res.: Earth Surf.* **118**, 497–518 (2013).
70. Wolf, S., Huisman, R., Muñoz, J., Curry, M. & van der Beek, P. Growth of collisional orogens from small and cold to large and hot-inferences from geodynamic models. *J. Geophys. Res.: Solid Earth* **126**, e2020JB021168 (2021).
71. Molnar, P. et al. Continuous deformation versus faulting through the continental lithosphere of New Zealand. *Science (New York, NY)* **286**, 516–519 (1999).
72. Molnar, P. & Tapponnier, P. Cenozoic tectonics of Asia: Effects of a continental collision. *Science* **189**, 419–426 (1975).
73. Whittaker, A. & Boulton, S. Tectonic and climatic controls on knickpoint retreat rates and landscape response times. *J. Geophys. Res.: Solid Earth* **117**, 2024 (2012).
74. Liu, Y. et al. Late Quaternary terrace formation from knickpoint propagation in the headwaters of the Yellow River, NE Tibetan Plateau. *Earth Surf. Process. Landf.* **46**, 2788–2806 (2022).
75. Braun, J. et al. Quantifying rates of landscape evolution and tectonic processes by thermochronology and numerical modeling of crustal heat transport using PECUBE. *Tectonophysics* **524**, 1–28 (2012).
76. Pan, G., Ding, J., Yao, D. & Wang, L. Geological map of the Qinghai-Xizang (Tibet) Plateau and adjacent areas, with guidebook. (2004).

Acknowledgements

This research is supported by National Natural Science Foundation of China (4201001, 41971005, 42272111) and Second Tibetan Plateau Scientific Expedition Program (2019QZKK0205, 2019QZKK0204). The University of Melbourne thermochronology laboratory receives support under the AuScope program (auscope.org.au) of the Australian Government's National Collaborative Research Infrastructure Strategy (NCRIS). For this study, sampling permissions were obtained. We thank the reviewers for their constructive suggestions for improving the manuscript and the editor, Joao Duarte, for professional editorial handling.

Author contributions

X.W. and G.L. developed the conceptual idea, designed and organized the study, and wrote the manuscript with D.C.; G.L. conducted fieldwork and processed data. X.W., G.L., and D.C. analyzed the data, tested the numerical simulations, and created all figures. X.W., G.L., D.C., R.J., B.K., W.Z., J.D.G. and H.L. discussed and revised early versions of the ideas. All authors contributed to the discussion and writing of the manuscript.

Competing interests

The authors declare no competing interests.

Additional information


Supplementary information The online version contains supplementary material available at <https://doi.org/10.1038/s43247-023-00861-y>.

Correspondence and requests for materials should be addressed to Xianyan Wang or Guangwei Li.

Peer review information *Communications Earth & Environment* thanks Erin Seagren, Luca Malatesta and the other, anonymous, reviewer(s) for their contribution to the peer review of this work. Primary Handling Editors: João Duarte and Joe Aslin. A peer review file is available

Reprints and permission information is available at <http://www.nature.com/reprints>

Publisher's note Springer Nature remains neutral with regard to jurisdictional claims in published maps and institutional affiliations.

 **Open Access** This article is licensed under a Creative Commons Attribution 4.0 International License, which permits use, sharing, adaptation, distribution and reproduction in any medium or format, as long as you give appropriate credit to the original author(s) and the source, provide a link to the Creative Commons licence, and indicate if changes were made. The images or other third party material in this article are included in the article's Creative Commons licence, unless indicated otherwise in a credit line to the material. If material is not included in the article's Creative Commons licence and your intended use is not permitted by statutory regulation or exceeds the permitted use, you will need to obtain permission directly from the copyright holder. To view a copy of this licence, visit <http://creativecommons.org/licenses/by/4.0/>.

© The Author(s) 2023